AGU PUBLICATIONS

JGR

Journal of Geophysical Research: Earth Surface

RESEARCH ARTICLE
10.1002/2014JF003085

**Key Points:**
- Density and size of ice wedges increase northward across tree line
- Properties of organic soils favor ice wedge development
- Moisture has contrasting effect on thermal regime of peat across tree line

**Supporting Information:**
- Readme
- Figure S1
- Table S1
- Table S2
- Table S3
- Table S4

**Correspondence to:**
S. V. Kokelj,
steve_kokelj@gov.nt.ca

**Citation:**
Kokelj, S. V., T. C. Lantz, S. A. Wolfe, J. C. Kanigan, P. D. Morse, R. Coutts, N. Molina-Giraldo, and C. R. Burn (2014), Distribution and activity of ice wedges across the forest-tundra transition, western Arctic Canada, *J. Geophys. Res. Earth Surf.*, *119*, 2032–2047, doi:10.1002/2014JF003085.

Received 8 JAN 2014
Accepted 16 AUG 2014
Accepted article online 24 AUG 2014
Published online 30 SEP 2014

# Distribution and activity of ice wedges across the forest-tundra transition, western Arctic Canada

**S. V. Kokelj[1,2,3], T. C. Lantz[2], S. A. Wolfe[4,3], J. C. Kanigan[5], P. D. Morse[4,3], R. Coutts[6], N. Molina-Giraldo[6], and C. R. Burn[3]**

[1]Northwest Territories Geoscience Office, Government of the Northwest Territories, Yellowknife, Northwest Territories, Canada, [2]School of Environmental Studies, University of Victoria, Victoria, British Columbia, Canada, [3]Department of Geography and Environmental Studies, Carleton University, Ottawa, Ontario, Canada, [4]Geological Survey of Canada, Natural Resources Canada, Ottawa, Ontario, Canada, [5]Cumulative Impact Monitoring Program, Environment and Natural Resources, Government of the Northwest Territories, Yellowknife, Northwest Territory, Canada, [6]Matrix Solutions Inc., Calgary, Alberta, Canada

**Abstract** Remote sensing, regional ground temperature and ground ice observations, and numerical simulation were used to investigate the size, distribution, and activity of ice wedges in fine-grained mineral and organic soils across the forest-tundra transition in uplands east of the Mackenzie Delta. In the northernmost dwarf-shrub tundra, ice wedge polygons cover up to 40% of the ground surface, with the wedges commonly exceeding 3 m in width. The largest ice wedges are in peatlands where thermal contraction cracking occurs more frequently than in nearby hummocky terrain with fine-grained soils. There are fewer ice wedges, rarely exceeding 2 m in width, in uplands to the south and none have been found in mineral soils of the tall-shrub tundra, although active ice wedges are found there throughout peatlands. In the spruce forest zone, small, relict ice wedges are restricted to peatlands. At tundra sites, winter temperatures at the top of permafrost are lower in organic than mineral soils because of the shallow permafrost table, occurrence of phase change at 0°C, and the relatively high thermal conductivity of icy peat. Due to these factors and the high coefficient of thermal contraction of frozen saturated peat, ice wedge cracking and growth is more common in peatlands than in mineral soil. However, the high latent heat content of saturated organic active layer soils may inhibit freezeback, particularly where thick snow accumulates, making the permafrost and the ice wedges in spruce forest polygonal peatlands susceptible to degradation following alteration of drainage or climate warming.

## 1. Introduction

Permafrost is integral to the stability of northern landscapes, ecosystems, and infrastructure. The sensitivity of permafrost terrain is controlled by ground thermal conditions and the nature and distribution of ground ice [*Mackay*, 1970]. Since the 1970s permafrost temperatures in the Canadian western Arctic have increased by 2 to 4°C in response to climate warming [*Smith et al.*, 2005; *Burn and Kokelj*, 2009; *Burn and Zhang*, 2009], and similar data have been collected in other parts of the circumpolar Arctic [*Romanovsky et al.*, 2010]. Rising ground temperatures are of particular relevance for ice-rich terrain where thawing can cause significant subsidence or lead to the release of soil carbon to the atmosphere [*Jorgenson et al.*, 2006; *Kokelj and Jorgenson*, 2013].

Polygonal ice wedge networks are common in areas of continuous permafrost [*Lachenbruch*, 1962; *Mackay*, 1963] (Figure 1a). Areas of polygonal terrain are considered sensitive to environmental disturbance and climate change because wedge ice is typically encountered near the top of permafrost (Figure 1b) [*Lachenbruch*, 1962; *Mackay*, 2000; *Jorgenson et al.*, 2006]. Rolling upland surfaces underlain by fine-grained soils near the Canadian western Arctic coast commonly host large epigenetic and antisyngenetic ice wedges several meters in width [*Pollard and French*, 1980; *Mackay*, 1995a], whereas thinner, syngenetic wedges are found in alluvial settings [*Mackay*, 1990; *Kokelj et al.*, 2007a; *Morse and Burn*, 2013].

Ice wedges (Figure 1b) develop in permafrost where winter temperatures are sufficiently low to cause thermal contraction cracking [*Lachenbruch*, 1962; *Mackay*, 1974]. Infiltration and refreezing of snowmelt forms a vein of ice in these cracks, and as this process is repeated, an ice wedge develops [*Lachenbruch*, 1962]. Air temperatures, snow accumulation, vegetation, and soil properties interact to influence the rates and magnitude

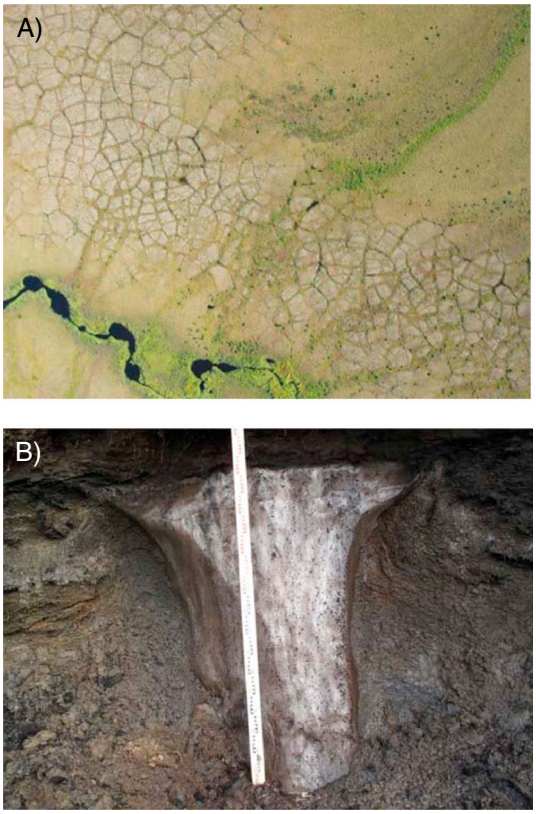


**Figure 1.** (a) Polygons and beaded stream, dwarf-shrub tundra, Mackenzie Delta region, western Arctic Canada. (b) Ice wedge exposed in the headwall of a thaw slump on Richards Island. The wedge is almost 2 m wide and is exposed to a depth of 2 m. The interface between wedge ice and the active layer is planar suggesting truncation by thawing.

of ground cooling and ice wedge development at local and regional scales [*Péwé*, 1966; *Romanovskii*, 1985; *Mackay*, 1993, 2000; *Fortier and Allard*, 2005; *Kokelj et al*., 2007a; *Watanabe et al*., 2013].

In the western Arctic, the ecological transition across tree line and variation in soil type lead to distinct differences in ground thermal regime [*Burn and Kokelj*, 2009; *Burn et al*., 2009; *Palmer et al*., 2012] and provide diverse settings for the development and preservation of wedge ice (Figure 2) [*Kokelj et al*., 2007a]. The objectives of this paper are to (1) investigate the distribution of polygonal terrain and the size of ice wedges in hummocky fine-grained mineral soils and peatlands across the low Arctic forest-tundra transition and (2) examine soil and permafrost conditions that control ice wedge development. Three working hypotheses provided the impetus for this research: (1) that the northward decrease in snow accumulation across the forest-tundra transition controls the frequency of thermal contraction cracking on a regional basis; (2) that spatially, conditions conducive to thermal contraction cracking are positively associated with a greater abundance and size of ice wedges; and (3) that soil physical properties are a secondary modulator of thermal contraction cracking, leading to distinct differences in the distribution and size of ice wedges in organic and hummocky fine-grained mineral soils. These hypotheses are tested with data on the distribution of ice wedge polygons determined from aerial photographs acquired in 2004, on the size of ice wedges exposed in cross section and determined by shallow drilling, and on the thermal regime of near-surface permafrost for organic and fine-grained mineral soils determined from extensive field investigations and numerical modeling.

## 2. Study Area

This paper focuses on the forest-tundra transition east of the Mackenzie Delta, NWT (Figure 2). The entire area was covered by Wisconsinan glacial ice between about 30 and 25 ka B.P. [*Duk-Rodkin and Lemmen*, 2000], and the predominant surficial materials are fine-grained and stony tills. Aeolian sands are common in the northwestern portion of Richards Island [*Dallimore et al*., 1997]. Lake drainage throughout the Holocene has resulted in extensive lacustrine basins which now contain polygonal peat plateaus [*Mackay*, 1992a; *Murton*, 1996; *Marsh et al*., 2009].

This lake-rich landscape is characterized by low, rolling hilly terrain interspersed by lacustrine plains that are locally dominant in the central and northern part of the study area [*Burn and Kokelj*, 2009]. The entire area is underlain by ice-rich permafrost [*Heginbottom et al*., 1995; *Burn and Kokelj*, 2009]. Near-surface segregated ice is common in the upper 2–3 m of the ground, above the early Holocene thaw unconformity [*Burn*, 1997; *Kokelj and Burn*, 2003; *Morse et al*., 2009]. Pleistocene deposits host thick bodies of segregated and buried glacier ice [*Mackay and Dallimore*, 1992; *Murton et al*., 2005]. Ice wedges are found throughout the region and are a principal reason for the high ice content of the uppermost 5 m of permafrost [*Pollard and French*, 1980].

Air temperatures are lower near the coast than inland, except in autumn and early winter, due to the persistence of sea ice in early summer and differences in the albedo of spruce forest and snow-covered

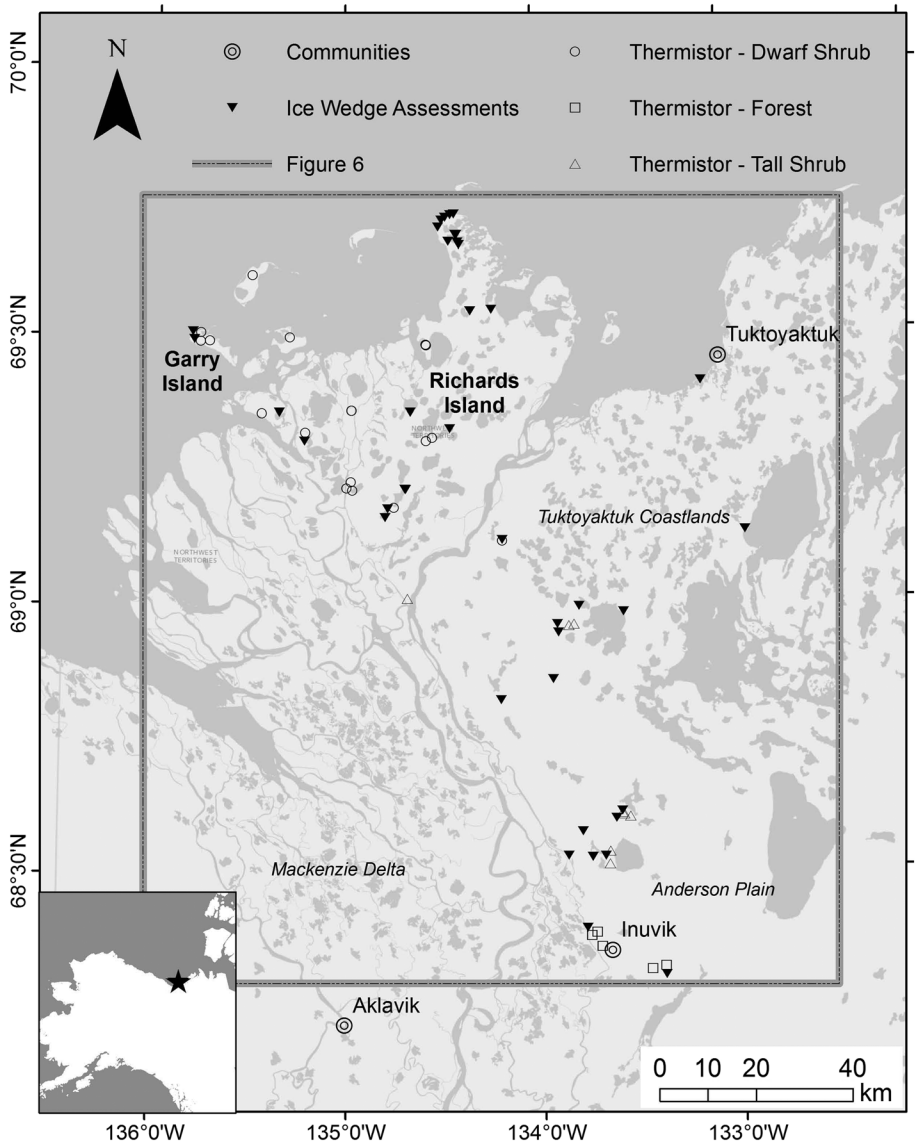


**Figure 2.** Map of the study region and study sites across the forest-tundra transition in the Tuktoyaktuk Coastlands and Anderson Plain.

tundra in late winter [*Burn and Kokelj*, 2009]. The mean annual air temperatures for 1971–2000 at Tuktoyaktuk and Inuvik were, respectively, −10.2°C and −9.0°C [*Environment Canada*, 2012]. The coast receives less precipitation than inland: annual snowfall for 1971–2000 at Inuvik was 57 cm, and 32 cm at Tuktoyaktuk. The ecological expression of this regional climatic gradient is a transition from open-canopy spruce forest near Inuvik to tall-shrub tundra in the central part of the study region to dwarf-shrub tundra near the Beaufort Sea coast [*Lantz et al.*, 2010]. The variation in regional mean ground temperatures is driven primarily by differences in snow depth across tree line [*Burn and Kokelj*, 2009; *Palmer et al.*, 2012]. Mean annual permafrost temperatures on the tundra uplands of Richards Island are as low as −7°C [*Burn and Kokelj*, 2009]. In the southern part of the study area, ground temperatures within the spruce forest range from −3 to −1°C, where deeper snow inhibits ground heat loss [*Kokelj et al.*, 2007a; *Burn et al.*, 2009; *Palmer et al.*, 2012]. Mean annual air temperature in the central Mackenzie Delta region has increased by an average of 2.2°C since 1926 [*Lantz and Kokelj*, 2008], but most of this warming has occurred since 1970 [*Burn and Kokelj*, 2009]. Over the last three decades, mean annual ground temperatures in the region have risen by 1 to 3°C [*Smith et al.*, 2005; *Burn and Kokelj*, 2009].

**Table 1.** Snow Depth and Minimum Temperatures at the Top of Permafrost at Hummocky Mineral Soil and Peatland Sites From the Dwarf-Shrub to the Spruce Forest Zone in Uplands East of Mackenzie Delta[a]

| Site | Latitude | Mean End of August Active Layer Thickness (SD) (cm) | Mean Snow Depth (SD) (cm) (Mar 2008) | Minimum $T_{ps}$ (°C) (2007–2008) | Total # of Ice Wedges Which Cracked ($N = 10$) 2007–2010 |
|---|---|---|---|---|---|
| Dwarf-shrub tundra mineral soil (T7_HT) | 69°18′38.27″N | 48.9 (8.7) | 22.9 (8.5) | −15.4 | ---------- |
| Dwarf-shrub tundra peatland (T7_IW) | 69°18′36.29″N | 31.1 (6.6) | 24.3 (19.2) | −18.8 | 1, 2, 2, 1 |
| Dwarf-shrub tundra mineral soil (T6_HT) | 69°07′05.01″N | 43.9 (12.1) | 37.9 (8.1) | −14.1 | ---------- |
| Dwarf-shrub tundra peatland (T6_IW) | 69°07′24.29″N | ---------- | 42.7 (14.7) | -------- | 2, 1, 1, 1 |
| Tall-shrub tundra mineral soil (T5_HT) | 68°57′23.22″N | 44.6 (14.7) | 39.1 (10.7) | −14.1 | ---------- |
| Tall-shrub tundra peatland (T5_IW) | 68°57′33.27″N | 36.0 (8.2) | 38.6 (18.5) | −14.8 | 1, 0, 1, 0 |
| Tall-shrub tundra mineral soil (T4_HT) | 68°36′29.95″N | 68.8 (25.2) | 45.3 (14.8) | −12.8 | ---------- |
| Tall-shrub tundra peatland (T4_IW) | 68°36′36.99″N | 33.1 (8.2) | 40.9 (15.3) | −14.7 | 0, 0, 1, 1 |
| Spruce forest mineral soil (T1_HT) | 68°21′45.38″N | 59.4 (9.8) | 74.9 (11.8) | −11.1 | ---------- |
| Spruce forest peatland (T1_IW) | 68°18′49.82″N | 58.4 (11.1) | 60.9 (15.2) | −0.61 | 0, 0, 0, 0 |

[a]Cracking conditions for peatland sites are also reported. The dashed line indicates that data were not collected.

## 3. Methods

This study was conducted to investigate the influence of latitude and soil type on the variation in near-surface thermal conditions and ice wedge development. We obtained all field data to test our research hypotheses on near-surface ground temperatures, ice wedge cracking, ice wedge characteristics, and distribution of polygonal terrain from the following vegetation zones, which characterize the forest-tundra and shrub-tundra ecotones: (1) Open-canopy spruce forest, (2) tall-shrub tundra, and (3) dwarf-shrub tundra [*Timoney et al.*, 1992; *Lantz et al.*, 2010]. Throughout the paper, we refer to these areas as the spruce forest zone, tall-shrub zone and dwarf-shrub zone, respectively. In each of these zones we selected sites in two soil types: (1) fine-grained mineral soils typically characterized by hummocky terrain and (2) organic soils which are associated with peatlands. These are the dominant soil types in the study region [*Rampton*, 1988].

We analyzed near-surface ground temperatures from a total of 34 locations in fine-grained mineral and organic soils distributed across the forest-tundra transition zone to describe regional variability in ground freezing and thermal conditions conducive to ice wedge cracking (Figure 2 and Table S1 in the supporting information). Sites were in flat terrain to avoid local effects of topography on snow and moisture conditions. We also monitored five core study sites in flat, undisturbed terrain, where snow depths, near-surface and deep ground temperatures and active layer thicknesses were assessed (Figure 2 and Table 1 and Table S1). At these locations, near-surface ground temperatures were measured in fine-grained hummocky soils, and in nearby peatlands where ice wedge cracking was also monitored (Table 1). Ice wedge characteristics were also assessed at 51 sites in fine-grained and organic soils from across this transition zone (Figure 2). Mapping of polygonal terrain focused on a 3739 $km^2$ area that extends across the forest-tundra transition and through the center of the region where ground temperatures and ice wedge conditions were assessed.

### 3.1. Thermal Conditions and Ice Wedge Cracking

Ground temperatures were measured from 2007 to 2009 at 34 sites across the forest-tundra transition, 24 in fine-grained mineral soils from hummocky terrain and 10 in organic soils from polygonal peatlands (Figure 2). Terrain with hummocky microtopography was characterized by organic-rich interhummock troughs, and hummocks composed of silty clay soils overlain by less than 0.2 m of organic materials. Active layer thickness ranged from 0.3 m in organic-filled troughs up to 1.2 m in bare hummock tops [*Kokelj et al.*, 2007b]. In peatlands, the active layer and near-surface permafrost consisted of moderately decomposed sedge and *Sphagnum* peat to depths of at least 1.5 m. The depth of maximum thaw in these organic soils was generally less than 0.6 m (Table 1).

Ground temperature measurements were made at 2 h intervals with thermistors (Onset Computing, HOBO™, TMC6-HA) connected to miniature data loggers (Onset Computing, HOBO™, H08-006-04). The temperature sensors had a range of −40 to 100°C, an accuracy of ±0.5°C and a precision of ±0.41°C at 0°C. In polygonal terrain, thermistors were situated in the ice wedge polygons and positioned at 0.05 m depth and in the top of permafrost. In fine-grained hummocky soils the thermistor at the top of permafrost was positioned at 1.0 m depth, however, in the peatlands where the active layer is typically shallower (Table 1), thermistors installed at the

top of permafrost were typically positioned at 0.7 m depth. Throughout this paper ground surface temperatures (0.05 m depth) are referred to using $T_s$ and temperatures at the top of permafrost are denoted by $T_{ps}$.

Using the ground temperature data from the 34 sites, the number of times that cooling rates and temperatures at the top of permafrost reached or exceeded ice wedge cracking thresholds was tallied. Thresholds were derived from previously published data [*Mackay*, 1993; *Allard and Kasper*, 1998; *Christiansen*, 2005; *Fortier and Allard*, 2005] for sites with organic soils which show that maximum $T_s$ at the time of ice wedge cracking are approximately −15°C and average 5 day rates of ground surface cooling prior to ice wedge cracking typically exceed 0.5°C $d^{-1}$. Near the permafrost table, the maximum temperature measured in association with ice wedge cracking has been approximately −13°C and cooling rates for periods of 5 days preceding cracking events are generally greater than 0.2°C $d^{-1}$ [*Mackay*, 1993; *Allard and Kasper*, 1998; *Fortier and Allard*, 2005].

Ice wedge cracking and snow depth were monitored from 2007 to 2009 at five polygonal peatlands (Figure 2 and Table 1) to examine regional and local controls on the activity of ice wedges. Ten ice wedges were monitored at each site to determine if thermal contraction cracking had occurred during the preceding winter. Thermal contraction cracking was assessed by burying a fine teflon coated wire (32 AWG) across troughs in summer and then checking for breakage in winter or the following spring [*Mackay*, 1974, 2000; *Fortier and Allard*, 2005]. Snow pits were excavated across each ice wedge in late March or early April to verify ice wedge cracking [*Mackay*, 1974], and snow surveys were conducted between each polygon center and ice wedge trough during these visits.

### 3.2. Mapping the Distribution of Polygonal Terrain

We used remote sensing to investigate regional variability in the distribution of polygonal terrain. Aerial photographs at 1:30,000 scale with a resolution of 0.5 m (Mackenzie Valley Air Photo Project, Department of Indian and Northern Affairs Canada, 2004) were used to map all areas of polygonal terrain (>100 $m^2$) within a 3739 $km^2$ study corridor that extended from spruce forest near Inuvik to dwarf-shrub tundra on Richards Island. Polygonal terrain on hill tops and in peatlands in open-canopy spruce forest and tundra environments can be effectively mapped using aerial photographs. Ice wedge polygons beneath closed canopy spruce forests in alluvial deposits of the Mackenzie Delta are also discernable using aerial photographs, although vegetation may obscure some features [*Kokelj and Burn*, 2004]. The orthorectified photographs were mosaicked to produce a digital map that covered the study region. Discrete areas of polygonal terrain were digitized on-screen in ArcGIS 9.3.1 and the area of each feature was calculated using Hawth's Tools 3.2.7. The Kernel Density tool in ArcGIS was used to express the percentage of each map unit occupied by polygonal terrain and to visualize variation in the density of ice wedge networks across the study area.

### 3.3. Ice Wedge Characteristics

A total of 51 sites in fine-grained mineral and organic soils were assessed to determine variation in the distribution and size of wedge ice across the forest-tundra transition. Exposures in thaw slumps ($n = 38$) and quarry pits ($n = 2$) were examined to determine the presence/absence of ice wedges and characteristics of the wedge ice. Field observations were limited to those exposures developed into low angled slopes (<5°) on primary terrain surfaces in order to reduce the possibility of assessing the geometry of syngenetic or antisyngenetic ice wedges [*Mackay*, 1990]. Ice wedge widths were also assessed by drilling in nine peatlands. Observations by *Mackay* [2000] provided additional data from Garry Island ($n = 2$). True ice wedge widths were estimated from the intersection angle of the primary axis of each exposed ice wedge with the exposed face. This was determined from the angle of foliations within the ice wedge and of the ice wedge trough in the undisturbed surface above the slump. The true width of the ice wedge was estimated with

$$b = \cos A \cdot c \quad (1)$$

where $c$ is the observed wedge width and $A$ is the angle of the ice wedge from the perpendicular to the exposed face.

The distance from wedge ice to the ground surface and to the top of permafrost, the width of the top of the wedge, the vertical height of the ice wedge, and the thickness of the overlying active layer were also recorded.

### 3.4. Thermal Modeling

One-dimensional geothermal simulations were used to investigate the influence of soil type and moisture on variation in thermal contraction cracking conditions across the forest-tundra transition zone. Sensitivity

analyses were conducted to explore the influence of moisture content and snow cover on active layer freezeback and temperatures at the top of permafrost for hypothetical scenarios with organic and mineral soils in warm and cold permafrost. The mean annual ground temperatures (MAGT) were −2.0 and −6.6°C, at warm and cold sites, respectively. These MAGTs are representative of undisturbed site conditions in the spruce forest and dwarf-shrub tundra environments of the study region [*Burn et al*., 2009; *Burn and Kokelj*, 2009; *Palmer et al*., 2012]. Geothermal simulations were performed using TEMP/W, (®Geo-Slope International Ltd.). Details on the mechanics and governing equations of this finite element geothermal model are accessible via the TEMP/W manual (http://www.geo-slope.com). The ground surface energy flux was calculated using a surface energy balance (SEB) model that originated with *Hwang* [1976] and was subsequently implemented and extended as a TEMP/W software add-on module by Ardent Innovation Inc. Our geothermal simulations and sensitivity analysis were conducted on four modeled base cases. The effect of varying active layer moisture conditions was examined for saturated mineral and organic soils in warm and cold permafrost, respectively. The added effect on ground temperatures of doubling the normal snow cover was investigated in a second suite of analyses.

The SEB model represents a simplification of energy exchange between the atmosphere and the ground surface and is described by in detail by *Hwang* [1976]. The model computes heat energy flow across the ground surface based on a sum of energy fluxes, including long- and short-wave radiation, convective cooling from wind and evapotranspiration. The governing equations and model sensitivity to varying seasonal or annual constants for albedo, the greenhouse factor and evapotranspiration are described by *Hwang* [1976]. In estimating net long-wave radiation leaving the surface (*QL*), we note that *Hwang* [1976] applied a greenhouse factor which is the ratio of the long-wave radiation returning from the atmosphere to the long-wave radiation originally leaving the surface. Net long-wave radiation (*QL*) leaving the surface is calculated as

$$QL = E\sigma T_{sur}{}^{4}(1 - G) \tag{2}$$

where $E$ = surface emissivity, $G$ = greenhouse factor, $\sigma$ = Stefan-Boltzmann radiation constant (= $5.67 \times 10^{-8}$ W/ m$^2 \cdot$ K$^4$), and $T_{sur}$ = surface temperature (K). The term (1-G) in equation (2) represents the amount of long-wave radiation emitted from the ground which is not reflected back to the ground from the atmosphere. Hwang demonstrated that the greenhouse factor used in the SEB model was relatively insensitive to changes over its range of seasonal variability and subsequently provided a constant greenhouse factor 0.83 for use in the modeling. Monthly potential evapotranspiration was estimated using the Thornthwaite formula [*Thornthwaite*, 1948] multiplied by a modification factor ($F$) that takes into account soil moisture and vegetation conditions. The evapotranspiration factor (dimensionless and varying between 0 and 1) is a fraction of the maximum potential evapotranspiration. The evapotranspiration factor is constant throughout the simulation; however, the maximum potential evapotranspiration varies as a function of air temperature and daylight hours. *Hwang* [1976] reports the effect of the evapotranspiration factor on maximum predicted thaw depths. Other constants particular for a ground surface type including winter and summer albedo can be estimated from published values [*Hwang*, 1976; *Andersland and Ladanyi*, 2004]. Model calibration to a known MAGT ensures that the model produces reasonable results for undisturbed terrain before variations are made for parametric studies. Sensitivity analyses are undertaken to ensure that small changes in albedo or evapotranspiration values do not result in significant changes to the modeling results [*Hwang*, 1976].

Mean monthly climate normals (1971–2000) for Inuvik A in the spruce forest zone and Tuktoyaktuk in the dwarf-shrub zone [*Environment Canada*, 2012] were used in the SEB model to calculate approximate ground thermal conditions in the warm and cold permafrost environments. The SEB modeling approach utilized data interpolated linearly between mean monthly values for input parameters to approximate average thermal conditions for a particular soil type and climate. Input parameters for the SEB calculations include monthly climatic normals for air temperature, wind speed, and snow cover, together with representative values for solar radiation (Table S2) [*Titus and Truhlar*, 1969], and summer and winter values for albedo and evapotranspiration (Table S3) [*Hwang*, 1976].

Since this approach is a simplification of energy exchange between the atmosphere and the ground surface, it does not reproduce small-scale temporal variation in ground surface temperatures. However, our simulations and sensitivity analyses are concerned with thermal conditions well below the penetration of diurnal temperature variation in fine-grained and organic soils which is dampened beyond about 30 cm below the ground surface [*Williams and Smith*, 1989; *Molina-Giraldo et al*., 2011]. Although this SEB approach

**Table 2.** Typical Physical Properties of Saturated and Unsaturated Organic and Silty Clay Soils[a]

| Soil Type | Specific Gravity | Porosity ($m^3/m^3$) | Saturation ($m^3/m^3$) | Volume Water Content | $K_u$ W/m·K | $K_f$ W/m·K | $C_u$ MJ/($m^3$·°C) | $C_f$ MJ/($m^3$·°C) |
|---|---|---|---|---|---|---|---|---|
| Silty clay Unsaturated | 2.7 | 0.46 | 0.50 | 0.23 | 0.90 | 1.00 | 1.9 | 1.5 |
| Silty clay Saturated | 2.7 | 0.46 | 1.00 | 0.46 | 1.27 | 1.97 | 2.9 | 1.9 |
| Organic Unsaturated | 1.4 | 0.78 | 0.50 | 0.39 | 0.20 | 0.30 | 1.9 | 1.2 |
| Organic Saturated | 1.4 | 0.78 | 1.00 | 0.78 | 0.45 | 1.00 | 3.4 | 1.9 |

[a]Frozen and unfrozen thermal conductivity is $K_u$ and $K_f$ and frozen and unfrozen volumetric heat capacity is $C_u$ and $C_f$, respectively. Representative values were obtained from *Andersland and Ladanyi* [2004].

is one of coarse granularity, the effectiveness is apparent as our simulations reproduce ground temperatures measured in the field (Figure S1), which are sufficient to drive our geothermal simulations and address our research questions. This approach is commonly implemented in geothermal modeling for pipeline design, freezeback of mine tailings, or drilling wastes and the performance of frozen core dams [*Nixon and Holl*, 1998; *Nixon*, 1998; *Kokelj et al.*, 2010; *Oswell*, 2011]. Our sensitivity analysis is concerned with the general behavior of active layer freezeback and the response of $T_{ps}$ for different soil profiles in warm and cold permafrost to variation in moisture and snow. The goal of the modeling was not to reconstruct ground surface conditions at a specific site for a particular year.

The use of an SEB boundary condition at the ground surface for thermal modeling has advantages over the *n*-factor approach [*Andersland and Ladanyi*, 2004] where the ground surface boundary temperature is the air temperature multiplied by empirical values for winter and summer conditions. With the SEB approach, energy fluxes at the ground surface are computed based on a variety of conditions and the ground surface temperatures are subsequently calculated. Furthermore, the SEB boundary condition enables investigation of variations in snow thickness on ground temperatures.

Calibration of the thermal simulations used climate normals and MAGT for each site. A transient one-dimensional thermal analysis performed in TEMP/W, using the SEB boundary condition at the ground surface was repeated using various snow thermal conductivity values until the model-computed MAGT matched the field-measured MAGT. The snow thermal conductivity value obtained from model calibration was 0.24 W/m·K and is within the range of measured values of 0.08 and 0.7 W/m·K for loose and compacted snow, respectively [*Andersland and Ladanyi*, 2004]. The calibrated snow thermal conductivity in the SEB model represents the average (or normal) snow thermal conductivity throughout the winters of multiple years.

The simulations assumed a two-layer soil profile with an organic thickness of 0.1 m or 2.0 m overlying a fine-grained mineral soil column to the depth of 30 m. These profiles represent general conditions in fine-grained soils and peatlands, respectively. The vertical node spacing in the finite element mesh was 0.025 m at the top of the profile and increased to approximately 1.0 m at the bottom. The material properties summarized in Table 2 were based on field determinations or representative values from *Andersland and Ladanyi* [2004]. The fraction of the total water content, $w$, that is unfrozen, $w_u$, was modeled as a function of temperature using

$$w_u = A(-T)^B \tag{3}$$

where A and B were −0.10 and −0.30 for mineral soils and −0.05 and −0.70 for organic soils, respectively.

The volumetric heat capacity of the soil, $c_v$, was calculated following *Andersland and Ladanyi* [2004]:

$$c_v = \left(\frac{\rho_d}{\rho_w}\right)\left(r_s + \frac{w_u}{100} + \frac{0.5w_i}{100}\right)c_w \tag{4}$$

where $\rho_d$ is the dry bulk density of soil, $\rho_w$ is the density of water, $r_s$ is the ratio of the heat capacity of the soil particles (0.18) or organic matter (0.4) to the heat capacity of water, $c_w$ (4.187 MJ/$m^3$·°C), $w_u$ is the water content, and $w_i$ is the ice content. The specific heat capacity of ice is approximately half that of water.

A series of modeling runs was performed first for calibration and then for the sensitivity analyses outlined in Table 3. Comparisons of modeled $T_s$ and $T_{ps}$ for the four climate and soil base cases (fine-grained and organic soils in spruce forest and low-shrub tundra zones), and corresponding field data are presented in Figure S1. These data illustrate that the modeling reasonably represents the near-surface thermal conditions that can be expected to characterize mineral and organic sites in the spruce forest and dwarf-shrub tundra zones of the

**Table 3.** Thermal Modeling Results Including Active Layer Thickness, Freezeback Duration, and Minimum Temperature at 1 m Depth[a]

| Site Type and Climate Zone | Mean $T_{ps}$ (°C) | Organic Soil Thickness (m) | Moisture Condition | Snow Depth Factor | Active Layer Thickness (m) | Freezeback Duration (Days) | Minimum Temperature at 1 m Depth (°C) |
|---|---|---|---|---|---|---|---|
| *Dwarf-Shrub Tundra* | | | | | | | |
| Peatland-dry | −6.6 | 2.0 | Unsaturated | 1 | 0.44 | 36 | −16.3 |
| Peatland-dry, 2X snow | −6.6 | 2.0 | Unsaturated | 2 | 0.44 | 46 | −14.2 |
| Peatland-wet | −6.6 | 2.0 | Saturated | 1 | 0.44 | 51 | −14.1 |
| Peatland-wet 2X snow | −6.6 | 2.0 | Saturated | 2 | 0.48 | 79 | −8.0 |
| Fine-grained-dry | −6.6 | 0.1 | Unsaturated | 1 | 0.73 | 21 | −15.8 |
| Fine grained-dry, 2X snow | −6.6 | 0.1 | Unsaturated | 2 | 0.76 | 26 | −11.9 |
| Fine grained-wet | −6.6 | 0.1 | Saturated | 1 | 0.70 | 31 | −13.0 |
| Fine grained-wet 2X snow | −6.6 | 0.1 | Saturated | 2 | 0.79 | 45 | −7.4 |
| *Spruce Forest* | | | | | | | |
| Peatland-dry | −2.0 | 2.0 | Unsaturated | 1 | 0.63 | 64 | −11.7 |
| Peatland-dry, 2X snow | −2.0 | 2.0 | Unsaturated | 2 | 0.62 | 104 | −7.6 |
| Peatland-wet | −2.0 | 2.0 | Saturated | 1 | 0.63 | 98 | −6.8 |
| Peatland-wet 2X snow | −2.0 | 2.0 | Saturated | 2 | n/a | [b]DNF | −0.34 |
| Fine grained-dry | −2.0 | 0.1 | Unsaturated | 1 | 1.22 | 54 | −10.3 |
| Fine grained-dry, 2X snow | −2.0 | 0.1 | Unsaturated | 2 | 1.27 | 69 | −5.2 |
| Fine grained-wet | −2.0 | 0.1 | Saturated | 1 | 1.17 | 64 | −5.8 |
| Fine grained-wet 2X snow | −2.0 | 0.1 | Saturated | 2 | 1.43 | 124 | −0.63 |

[a]Results are for the first year following modification of moisture and/or snow conditions from the initial calibrated base cases. Snow depth simulations were applied to the respective soil moisture scenarios after a 5 year period by which time the near-surface conditions had reached a periodic steady state.
[b]Active layer did not completely freeze.

study region. The model-computed active layer thicknesses were also compared with field measurements from peatlands and hummocky fine-grained mineral soils in the northern spruce forest and dwarf-shrub zones, respectively (Table 1) [*Kokelj et al.*, 2007b; *Burn and Kokelj*, 2009]. The comparison of simulated ground thermal conditions with field data demonstrates that the modeling methodology we implement is adequate to meet the objectives of our geothermal sensitivity analyses.

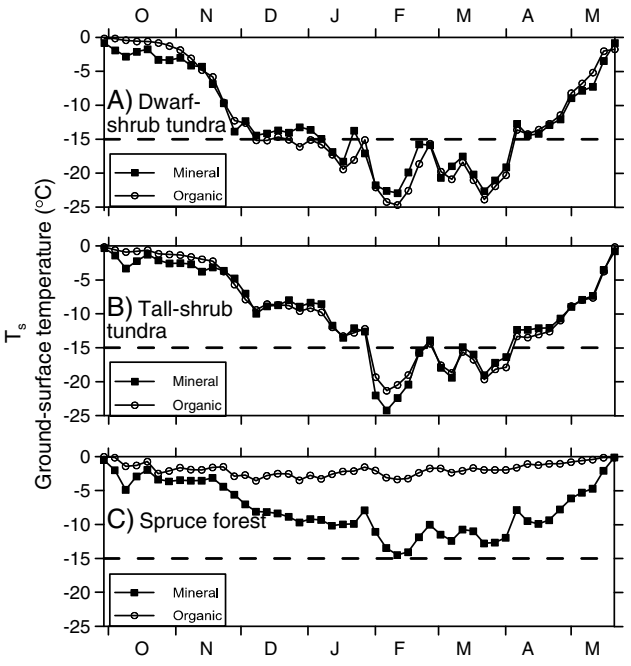


**Figure 3.** Ground surface temperatures ($T_s$; 5 cm depth) for mineral soil in hummocky uplands and organic soil in polygonal peatlands in the dwarf-shrub tundra (T7_HT; T7_IW), tall-shrub tundra (T4_HT; T4_IW), and the spruce forest (T1_HT; T1_IW) zones, October 2007 to May 2008, Mackenzie Delta region. The dashed line represents the cracking threshold temperature for the ground surface. The time series represents daily mean temperatures and symbols are plotted once every 5 days for clarity.

The theoretical base cases representing each saturated soil profile (mineral and organic) and climate combination (Inuvik and Tuktoyaktuk) were run until periodic steady state was reached. Subsequently, the influence of varying moisture content and snow cover on active layer freezeback and minimum $T_{ps}$ for the different soil types and climate conditions were investigated (Table 3). We report results of the sensitivity analyses taken from the second winter following the change in soil moisture conditions. Snow depth increases were applied to the respective soil moisture scenarios after the near-surface conditions had reached a steady state.

## 4. Results

### 4.1. Near-Surface Ground Cooling Conditions Across the Forest-Tundra Transition

In the dwarf-shrub zone, fine-grained soils in hummocky terrain and peatlands were

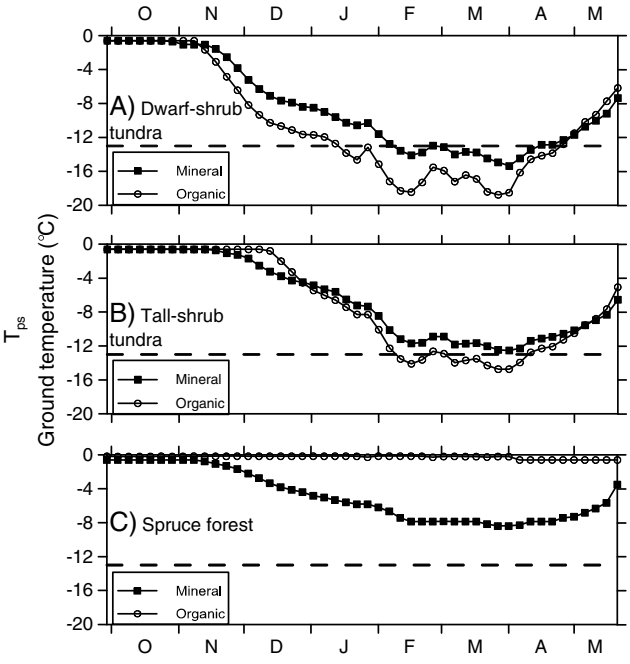


**Figure 4.** Ground temperatures at the top of permafrost ($T_{ps}$) for mineral soil in hummocky uplands and organic soil in polygonal peatlands in the dwarf-shrub tundra (T7_HT; T7_IW), tall-shrub tundra (T4_HT; T4_IW), and the spruce forest (T1_HT; T1_IW) zones, October 2007 to May 2008, Mackenzie Delta region. The dashed line represents the cracking threshold temperature at the top of permafrost. The time series represents daily mean temperatures and symbols are plotted once every 5 days for clarity.

characterized by thin snow cover and rapid active layer freezeback followed by an abrupt decrease in $T_s$ (Table 1 and Figures 3a and 4a) [*Burn and Kokelj*, 2009]. Mean end of March snow depths at these sites were less than 0.25 m in 2008 (Table 1). $T_{ps}$ declined more rapidly over the winter in the peatland than at the mineral soil site reaching minimum values of −18.8 and −15.4°C, respectively (Figure 4a). However, the rates and magnitude of cooling at the ground surface were similar at the two sites (Figure 3a).

In the tall-shrub zone, late winter snow cover was deeper and minimum ground temperatures were higher than at sites in the dwarf-shrub zone (Table 1 and Figures 3 and 4). The mean snow depths in late March 2008 were 0.41 m at the peatland in the tall-shrub tundra zone and 0.45 m at the nearby mineral soil site (Table 1). Although $T_s$ were similar at these sites (Figure 3b), the thicker active layer in the fine-grained mineral soil was frozen, as indicated by a decrease in $T_{ps}$ (Figure 4b), almost 2 weeks earlier than in the adjacent peatland (4 and 17 December). $T_s$ at the two sites in the tall-shrub tundra zone were similar following active layer freezeback (Figure 3b), but $T_{ps}$ at the peatland decreased more rapidly and the minimum temperatures recorded were lower than in the hummocky mineral soil (Figure 4b and Table 1).

The deepest snow and the highest winter ground temperatures were recorded at sites in the spruce forest zone (Table 1). Although the timing of active layer freezeback in 2007–2008 was similar at the forested site with fine-grained soils and the sites in the tall-shrub zone, $T_s$ and $T_{ps}$ at the fine-grained mineral soil forested site remained several degrees higher throughout the winter (Figures 3 and 4). $T_{ps}$ at the peatland in the spruce forest zone remained close to 0°C, and $T_s$ fell to just a few degrees below 0°C in winter 2007/2008. The persistence of unfrozen organic soils throughout winter was corroborated by drilling at a polygon trough in late March 2006 where a thin layer of thawed, saturated peat was found below 0.7 m of frozen soil. Ice wedge troughs at the polygonal peatlands are characterized by saturated organic soils and typically accumulate thicker snow than the adjacent polygon centers.

### 4.2. Thermal Modeling Results

Geothermal simulations confirm that an active layer in organic soils takes longer to freezeback than in mineral soils (Table 3). However, under comparable conditions, once frozen, ground temperatures at 1 m depth decline more rapidly in organic soils and therefore, reach lower minimum temperatures (Table 3). For the tundra scenarios, the simulations indicate that freezeback of organic soils took 15 to 34 days longer than for mineral soils, but subsequently, minimum temperatures at 1 m depth were 0.6 to 2.3°C lower than in comparable mineral soil simulations. For the spruce forest scenarios, freezeback took up to several months longer and minimum ground temperatures were higher than in the analogous tundra scenarios (Table 3). The influence of moisture had a much greater impact on freezeback duration in organic soils than in mineral soils with the most significant increases occurring in a warm permafrost setting where saturated organic material and a doubling of snow cover prevented the active layer from refreezing (Table 3).

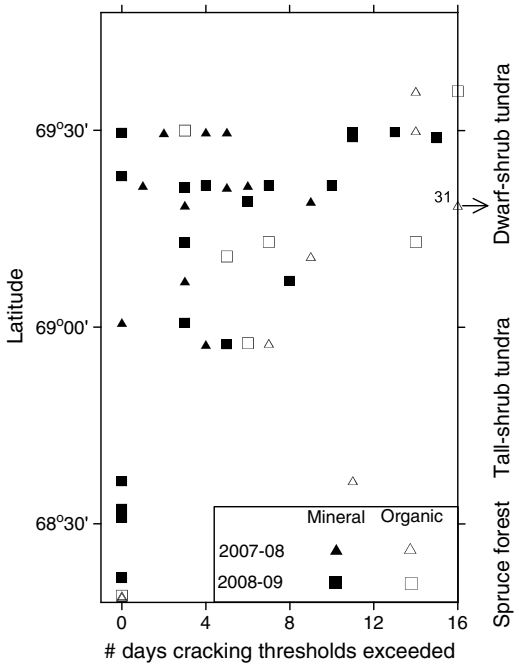


**Figure 5.** Number of days when ice wedge cracking thresholds were reached for sites across the study area, winter 2007–2008 and 2008–2009.

### 4.3. Regional Ice Wedge Cracking Thresholds

Cracking thresholds were reached several times each winter (2007/2008 and 2008/2009) at all fine-grained hummocky and peatland sites in the dwarf-shrub and northern tall-shrub zones, but the frequency varied substantially between sites and years (Figure 5). Thresholds were exceeded most often at sites north of 69°20′N, and the frequency of cracking in peatlands was often greater than in mineral soils of the nearby hummocky terrain (Figure 5). In winter 2007/2008, cracking thresholds were reached 31 times at a northern dwarf-shrub peatland but only 3 times in the nearby hummocky terrain (Figure 5). During the same winter, cracking thresholds were recorded 11 times at a peatland in the southern tall-shrub tundra zone (68°36′36″N) but were not reached in the nearby hummocky terrain (Figure 5) nor on adjacent slopes with dense alder stands. Ice wedge cracking thresholds were not reached at sites in the spruce forest zone, regardless of terrain type or year.

### 4.4. Ice Wedge Activity in Polygonal Peatlands

The frequency of ice wedge cracking varied among sites and years, but in general, ice wedges at the more northerly sites cracked regularly, whereas there was no indication of cracking at peatlands in the spruce forest zone (Table 1). The same ice wedge(s) generally cracked repeatedly. These active wedges were characterized by subtle troughs and low snow cover. In the spruce forest peatland, the ice wedge troughs are prominent features that are rectangular in cross section. None of these ice wedges were active during the study period, as also reported from a similar site less than 1 km away by *Mackay* [2000].

### 4.5. Distribution of Polygonal Terrain

Examination of aerial photographs showed that the proportion of the land surface covered by polygonal terrain increases with latitude, ranging from 5% in the south to 20–40% in the north (Figure 6). Thirty-three percent of the polygonal terrain was in lacustrine plains, and although 64% is associated with glaciofluvial and morainal deposits, many of the polygons in these areas occur in isolated lacustrine units that are too small to have been represented on the 1:250,000 scale maps presented by *Aylsworth et al.* [2000]. The proportion of the landscape covered by lacustrine sediments increased with latitude [*Aylsworth et al.* 2000].

### 4.6. Size and Distribution of Ice Wedges

The size and distribution of ice wedges varied across the forest-tundra transition with the largest and most abundant wedges occurring in the dwarf-shrub tundra. North of 69°00′N, ice wedges were observed in all 15 thaw slump exposures eroding primary upland surfaces in fine-grained ice-rich tills (Figures 6 and 7a). In this part of the study region, 39 wedges were observed in 850 m of exposure in 15 slumps. The largest wedges in hummocky fine-grained soils, over 3 m wide, were observed on Garry Island by *Mackay* [1963, 2000]. In hummocky terrain, ice wedges wider than 2 m were only observed north of 69°20′N, whereas maximum wedge widths less than 1 m were typical in exposures between 69°20′N and 69°00′N (Figure 8). Wedge ice is much less abundant in hummocky terrain through the tall-shrub tundra zone (Figures 6 and 8), where no ice wedges were observed in 10 discrete permafrost sections that were, in total, more than 1000 m long (Figure 7b). In the tall-shrub and spruce forest zones, polygonal terrain was restricted to organic deposits associated with lacustrine basins.

Shallow drilling confirmed that wedge ice is present in peatlands throughout the entire study region [*Mackay*, 2000; *Kokelj et al.*, 2007a]. These ice wedges are large in comparison to the wedges in fine-grained hummocky terrain. For example, at a peatland in dwarf-shrub tundra near Tuktoyaktuk several ice wedges greater than 3 m

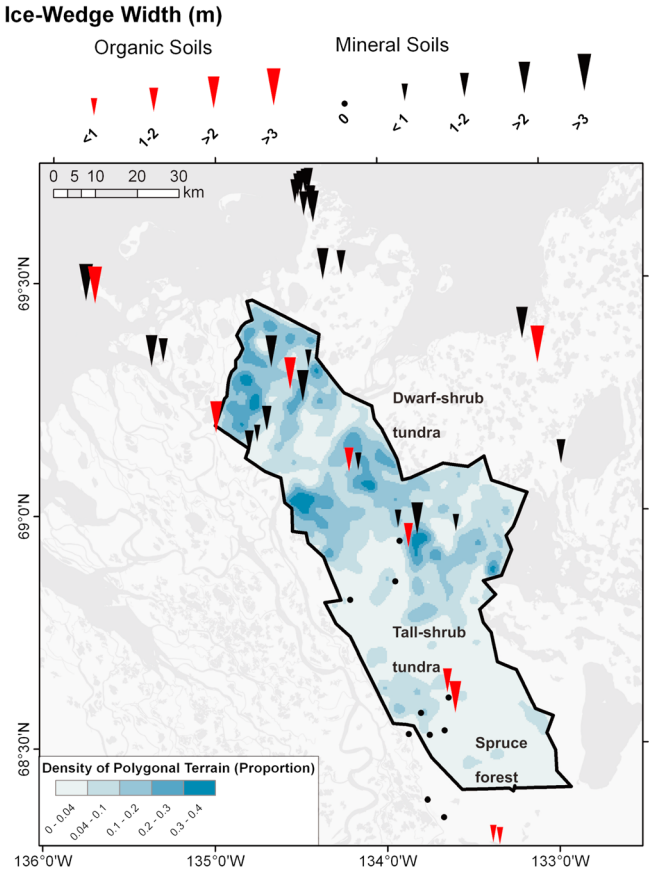


**Figure 6.** Density of polygonal terrain in the forest-tundra transition study area and wedge ice characteristics as determined by observations of thaw slump exposures in mineral soil uplands and by drilling in peatlands. Dots indicate thaw slump exposures in primary upland surfaces where wedge ice was not observed.

wide were delineated (Figures 6 and 8). Ice wedges in peatlands located in the southern tall-shrub zone were up to 2 m wide at the base of the active layer. In contrast, there was no wedge ice in nearby hummocky terrain (Figures 6 and 8). The 10 ice wedges drilled in the spruce forest peatland were less than 1 m wide and were all encountered 1.2 to 1.9 m below the trough surface, or 0.5 to 1.2 m below the depth of maximum thaw in the ice wedge troughs.

## 5. Discussion

### 5.1. Regional Ground Temperatures and Thermal Contraction Cracking Conditions Across the Forest-Tundra Transition

The northward decline in minimum ground temperatures with decreasing snow accumulation and shrub height and density [*Burn and Kokelj*, 2009; *Lantz et al.*, 2010; *Palmer et al.*, 2012] influenced regional variation in thermal contraction cracking (Figures 3–5 and Table 1), supporting our first working hypothesis. The lowest $T_s$ and $T_{ps}$ and greatest frequency of thermal contraction cracking were recorded at the most northerly sites in dwarf-shrub tundra (Table 1). Ground temperatures in winter were higher at sites in the tall-shrub zone than in the dwarf-shrub zone due to the greater snow depth; however, thermal conditions conducive to cracking were also observed during some years at polygonal peatlands in the tall-shrub zone suggesting that these environments contain moderately active ice wedges (Figures 3 and 4 and Table 1)

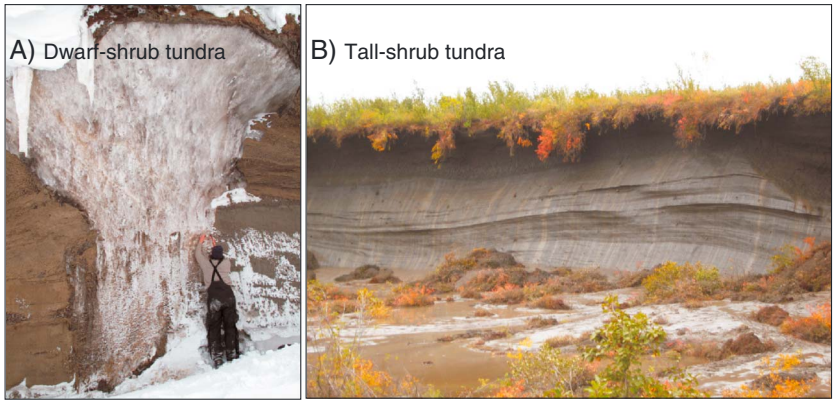


**Figure 7.** (a) Large ice wedge in a thaw slump exposure, dwarf-shrub tundra (69°21′25″N, 135°20′38″W). (b) Large thaw slump exposure into a primary upland surface showing no evidence of wedge ice, southern tall-shrub tundra zone (68°31′45″N, 133°44′35″W).

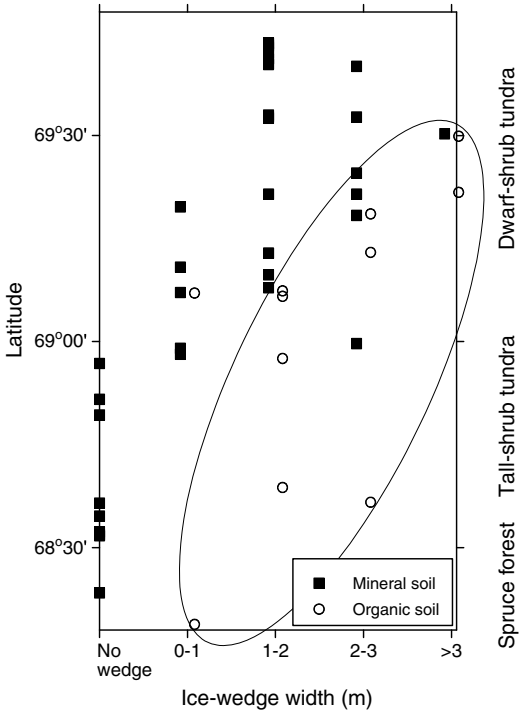


**Figure 8.** Maximum observed ice-wedge width for permafrost exposures in fine-grained tills and for polygonal peatlands in the Mackenzie Delta region. The ellipse encloses the majority of the peatland sites.

[*Mackay*, 1992b]. Thick snow accumulation in the spruce forest zone increased the duration of active layer freezing (Figures 3 and 4) and prevented conditions necessary for thermal contraction cracking (Figure 5). Long-term field observations by *Mackay* [2000] and isotope data [*Kokelj et al.*, 2007a] confirm that peatlands in the spruce forest zone contain inactive ice wedges.

### 5.2. Latitudinal Variation in the Size and Distribution of Ice Wedges

Our field data support the hypothesis that regional variation in the size and distribution of wedge ice follows latitudinal trends in shallow winter ground temperature and conditions conducive to thermal contraction cracking (Figures 5–8). Polygonal terrain and large ice wedges, some exceeding 3 m in width, were found throughout the dwarf-shrub tundra (Figures 6, 7, and 9). The size and abundance of ice wedges decreased in fine-grained soils of hummocky terrain in the tall-shrub zone, but ice wedges were abundant in peatlands throughout this zone (Figures 8 and 9). Peatlands in the spruce forest zone contained relict ice wedges that were less than 1 m wide (Figure 8) and were truncated well below the base of the contemporary permafrost table due to past thaw, possibly as a result of forest fire [*Mackay*, 1995b]. Regional variation in the distribution and size of ice wedges is consistent with a southward increase in mean annual ground temperature and a decrease in the frequency that thermal contraction cracking temperature thresholds are exceeded (Figure 5), both of which occur with increasing shrub height and density, and snow depth [*Kokelj et al.*, 2007a; *Lantz et al.*, 2010; *Palmer et al.*, 2012].

Taken together, these observations indicate that potential for terrain modification from ice wedge degradation due to climate warming or environmental disturbance is greatest in the dwarf-shrub tundra where much of the terrain is underlain by large ice wedges. However, the peatlands located in the spruce forest zone are most susceptible to thermal degradation because the duration of active layer freezeback approaches the length of the freezing season (Figure 4 and Table 3). The ice wedges in spruce forest peatlands are already relict features

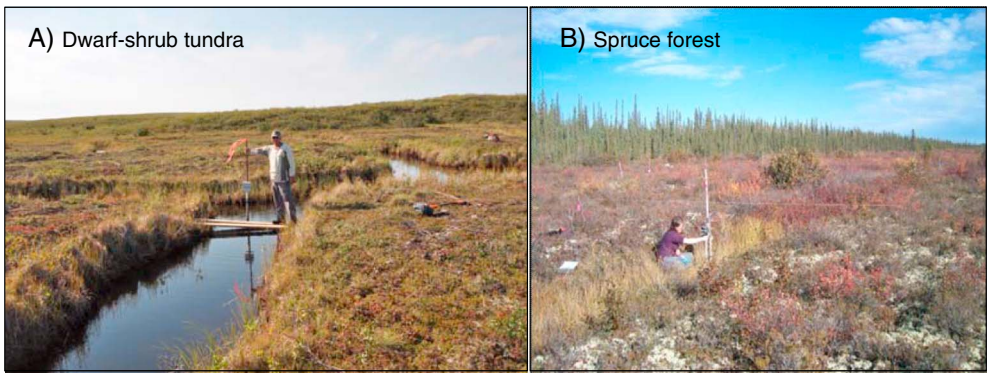


**Figure 9.** Trough development associated with degradation of ice wedges at (a) a dwarf-shrub tundra peatland underlain by large ice wedges and (b) a spruce forest peatland underlain by small ice wedges. Wedge ice was encountered immediately beneath the active layer at the dwarf-shrub tundra peatland. Wedge ice at the spruce forest peatland was truncated 50 to 100 cm beneath the permafrost table.

truncated in some cases up to a meter below the permafrost table. Unlike the large wedges in the dwarf-shrub tundra zone which are close to the permafrost surface, the thawing of wedges in the spruce forest peatlands would not occur immediately, and due to their small size, would have relatively minor impacts on surface subsidence and terrain modification.

### 5.3. The Influence of Soil Type on Ice Wedge Distribution Across the Forest-Tundra Transition

The abundance of wedge ice in peatlands throughout the study region indicates that soil type is an important modulator of thermal contraction cracking and ice wedge development, as suggested by our third working hypothesis. In the dwarf-shrub tundra, both organic and fine-grained mineral soils contain large ice wedges, and cracking thresholds were typically reached more frequently in peatlands than in the adjacent fine-grained hummocky tundra (Figures 5 and 8). However, in the southern tall-shrub tundra, wedge ice was restricted to peatlands where organic soils experienced conditions conducive to thermal contraction cracking (Figures 5 and 6 and Table 1). Peatlands in the spruce forest zone were the most southerly terrain with wedge ice, although these wedges were inactive (Figures 7 and 8) [*Kokelj et al.*, 2007a]. Wedge ice was not observed in any thaw slump exposures in mineral soils through the southern tall-shrub tundra or in the spruce forest zone (Figure 8).

Several characteristics of frozen organic soils favor thermal contraction cracking. First, the thermal stresses that cause ice wedge cracking originate at the top of permafrost [*Mackay*, 1974]. Peatlands are characterized by a shallow active layer due to the low thermal conductivity of thawed peat, evapotranspiration from the moss-covered surface, and high latent heat in saturated frozen peat (Tables 2). The permafrost table in organic soils is close to the ground surface, and following freezeback, may be subject to greater rates of ground cooling and lower minimum temperatures than in mineral soils where the permafrost table is typically deeper (Figure 4 and Tables 1 and 3). Second, the nature of soil freezing differs between organic and fine-grained mineral soils due to the higher unfrozen water content of fine-grained soils [*Williams and Smith*, 1989]. In organic soils, most soil water freezes close to 0°C so that latent heat effects are constrained to temperatures just below 0°C. When organic soils have frozen, further ground heat loss results in a rapid decline of $T_{ps}$ and the generation of thermal stress in the active layer and near-surface permafrost. In contrast, in fine-grained soils latent heat effects are distributed over 2–5°C below 0°C [*Kokelj and Burn*, 2003], thereby reducing the cooling rates of frozen ground [*Williams and Smith*, 1989]. Furthermore, the progressive freezing of pore water in fine-grained substrate contributes to thermal expansion of soils at temperatures several degrees below 0°C [*Andersland and Ladanyi*, 2004].

The potential for thermal contraction cracking in organic soils is also increased by the high volumetric water content of frozen peat and the high thermal contraction coefficient of ice [*Al Moussawi*, 1988; *Andersland and Ladanyi*, 2004]. The low bulk density and high porosity of saturated peat accommodates significantly greater volumes of soil water than in fine-grained mineral soils (Table 2). The coefficient of thermal contraction for ice at temperatures ranging from 0 to −40°C is approximately $5 \times 10^{-5}$ (°C)$^{-1}$ [*Andersland and Ladanyi*, 2004]. As this value is 3 to 5 times greater than for dry or saturated quartz sand, the thermal stresses generated in frozen, saturated organic soils would be significantly greater than in saturated mineral soils even if the rates of temperature decline were similar.

### 5.4. Contrasting Thermal Sensitivity of Organic and Mineral Soils

Our results show that soil moisture has an important influence on thermal properties in organic soils and can explain why the differences in ground temperatures north and south of tree line were greater in peatlands than in fine-grained mineral soils (Figure 4). The top of permafrost in peatlands in the dwarf-shrub zone was colder and more responsive to variations in air temperature than in nearby hummocky terrain (Figure 4a), although $T_s$ and snow depths were similar at these sites (Figure 3a and Table 1). In the tall-shrub zone where the snow cover was deeper, freezeback duration in the peatland was greater than in hummocky fine-grained soils likely because of a saturated organic active layer. However, once the peatlands had frozen, the rate of temperature decline at the top of permafrost exceeded the rates at mineral soil sites due to the high thermal conductivity of saturated frozen peat, the concentration of soil moisture freezing at 0°C in peat, and the shallower permafrost table in organic soils. These observations are corroborated by numerical analyses simulating ground thermal conditions in a tundra environment, which indicate that the duration of freezeback for an organic active layer is greater than for a mineral soil, but subsequent rapid cooling of organic soils leads to lower minimum ground temperatures in the peatlands (Table 3). Taken together, these observations suggest that the top of permafrost in

tundra peatlands can be more responsive to variations in air temperature in winter than the fine-grained hummocky upland sites because of contrasting subsurface thermal properties and active layer thicknesses, rather than to differences in snow thickness alone. These analyses also support the observations that wedge ice is more widely distributed in peatlands across the study region than in fine-grained soils.

In contrast with the tundra sites, the spruce forest peatlands were significantly warmer than nearby fine-grained forest soils despite similarly deep snow cover (Figures 3 and 4 and Table 1). At peatlands south of tree line, the high volumetric water content of a saturated organic soil in conjunction with a thick snow cover can inhibit active layer freezeback under contemporary conditions (Figure 4 and Table 3). Fine-grained forest soils, which contain less water by volume and have a higher thawed thermal conductivity than the organic soils are typically frozen by December or January. The thermal regime of fine-grained mineral soils is less influenced by changing soil moisture conditions because the latent heat content of saturated fine-grained soils is lower than that of organic soils (Table 2). Thermal analyses confirm that under most conditions, minimum $T_{ps}$ of organic soils is lower than in fine-grained soils even though freezeback duration is significantly greater (Table 3). However, the long freezeback of saturated organic soils indicates that under climate warming or increased snow cover, permafrost in the peatlands, which typically host wedge ice, may start to degrade before permafrost in mineral soils (Figures 3 and 4 and Table 3).

The presence of relict wedge ice in spruce forest peatlands also indicates the thermal sensitivity of organic soils. Long-term monitoring [*Mackay*, 2000], stratigraphic and isotopic evidence [*Kokelj et al*., 2007a], indicates that ice wedges in the spruce forest zone have been inactive for at least several decades. During colder or drier periods, such as the Little Ice Age, ground thermal conditions in spruce peatlands must have been conducive to the growth of ice wedges. During this period, ground temperatures were likely similar then to those recorded in peatlands of the southern tall-shrub tundra zone where ice wedges are presently active (Figure 4b and Table 1) [*Kokelj et al*., 2007a].

## 6. Conclusions

Based on our results and interpretations, we draw the following conclusions:

1. The latitudinal increase in thermal contraction cracking is associated with the northward decline in ground temperatures with decreasing snow accumulation across the forest-tundra transition.
2. The density of polygonal terrain and the size of ice wedges increases with latitude across the forest-tundra transition following the increase in ground thermal conditions conducive to ice wedge cracking. Cold climate conditions and thin snow cover are associated with frequent thermal contraction cracking, large ice wedges, and widespread polygonal terrain in the dwarf-shrub tundra. The absence of ice wedges from fine-grained mineral soils of the tall-shrub zone contrasts with the abundance of active ice wedges in peatlands. In the spruce forest zone, small, relict ice wedges are restricted to peatlands.
3. The contrasting thermal and physical properties of peat and mineral soils influence the distribution of wedge ice across the forest-tundra transition. Ice wedges are present in peatlands throughout the study region, but there is an abrupt southward decline in the abundance of wedge ice in fine-grained soils indicating that under low snow cover and cold climate conditions, organic deposits are more susceptible to thermal contraction cracking than fine-grained mineral soils. The association of peatlands with ice wedges is mainly because the volumetric water content of frozen peat is at least twice that of saturated fine-grained mineral soil and the thermal contraction coefficient of ice is 3–5 times greater than for mineral substrate.
4. Moisture may have a contrasting influence on the ground thermal regime of organic soils north and south of tree line. In dwarf-shrub tundra with thin snow cover, saturated organic soils freeze relatively early in the winter and their high ice content, with high thermal conductivity, favors ground heat loss and thermal contraction cracking. However, in the spruce forest zone, where the snow cover is relatively deep, the high latent heat content of the saturated organic active layer inhibits soil freezing in winter, and ground temperatures sufficient for thermal contraction cracking have not been recorded. The longer duration of active layer freezeback in organic soils indicates that under warmer climate or thicker snow conditions, terrain characterized by saturated organic soils may be the first to experience permafrost degradation. The persistence of unfrozen organic soils in ice wedge troughs at the end of winter, $T_{ps}$ which remain just below 0°C throughout winter, and truncation of wedge ice up to 1.5 m below the peatland surface indicates that ice wedges in subarctic peatlands are already degrading.

**Acknowledgments**

This research has been supported by the Cumulative Impact Monitoring Program, Aboriginal Affairs, and Northern Development Canada; the Natural Sciences and Engineering Research Council of Canada through grants to T.C. Lantz and a Northern Research Chair held by C.R. Burn; the Polar Continental Shelf Project (PCSP); the Climate Change Geoscience Program and the Program for Energy Research and Development of Natural Resources Canada; and the Aurora Research Institute. Field assistance from Douglas Esagok is gratefully acknowledged. We thank Sharon Smith, Michel Allard, the Associate Editor and two anonymous reviewers for helpful comments which have improved this manuscript. This paper is Northwest Territories Geoscience Office contribution 76 and NRCan contribution 20130468.

## References

Al Moussawi, H. (1988), Thermal contraction and crack formation in frozen soil, PhD thesis, Dept. of Civil and Environmental Eng., Michigan State Univ., East Lansing, Michigan.

Allard, M., and J. N. Kasper (1998), Temperature conditions for ice-wedge cracking: Field measurements from Salluit, northern Quebec, in *Proceedings of the 7th International Conference on Permafrost*, pp. 5–12, Cent. d'études nordiques, Univ. Laval, Ste.-Foy, Québec, Canada.

Andersland, O. B., and B. Ladanyi (2004), *Frozen Ground Engineering*, 2nd ed., John Wiley, Hoboken, N. J.

Aylsworth, J. A., M. M. Burgess, D. T. Desrochers, A. Duk-Rodkin, and J. A. Traynor (2000), Surficial geology, subsurface materials, and thaw sensitivity of sediments, in *The Physical Environment of the Mackenzie Valley, Northwest Territories: A Base Line for the Assessment of Environmental Change*, GSC Bulletin, vol. 547, pp. 41–48.

Burn, C. R. (1997), Cryostratigraphy, paleogeography, and climate change during the early Holocene warm interval, western Arctic coast, Canada, *Can J. Earth Sci.*, *34*, 912–925, doi:10.1139/e17-076.

Burn, C. R., and S. V. Kokelj (2009), The environment and permafrost of the Mackenzie Delta area, *Permafrost Periglac.*, *20*, 83–105, doi:10.1002/ppp.655.

Burn, C. R., and Y. Zhang (2009), Permafrost and climate change at Herschel Island (Qikiqtaruq), Yukon Territory, Canada, *J. Geophys. Res.*, *114*, F02001, doi:10.1029/2008JF001087.

Burn, C. R., J. R. Mackay, and S. V. Kokelj (2009), The thermal regime of permafrost and its susceptibility to degradation in upland terrain near Inuvik, N.W.T, *Permafrost Periglac.*, *20*, 221–227, doi:10.1002/ppp.649.

Christiansen, H. H. (2005), Thermal regime of ice-wedge cracking in Adventdale, Svalbard, *Permafrost Periglac.*, *16*, 87–98, doi:10.1002/ppp.523.

Dallimore, S. R., S. A. Wolfe, J. V. Matthews Jr., and J.-S. Vincent (1997), Mid-Wisconsinan eolian deposits of the Kittigazuit Formation, Tuktoyaktuk Coastlands, Northwest Territories, Canada, *Can. J. Earth Sci.*, *34*(11), 1421–1441, doi:10.1139/e17-116.

Duk-Rodkin, A., and D. S. Lemmen (2000), Glacial history of the Mackenzie region, in *The Physical Environment of the Mackenzie Valley, Northwest Territories: A Base Line for the Assessment of Environmental Change*, GSC Bulletin, vol. 547, pp. 11–20.

Environment Canada (2012), National Climate Data and Information Archive. [Available at http://climate.weatheroffice.gc.ca/climateData/canada_e.html.]

Fortier, D., and M. Allard (2005), Frost-cracking conditions, Bylot Island, eastern Canadian Arctic archipelago, *Permafrost Periglac.*, *16*, 145–161, doi:10.1002/ppp.504.

Heginbottom, J. A., M. A. Dubreuil, and P. A. Harker (1995), Canada—Permafrost, in *National Atlas of Canada*, 5th ed., MCR 4177, National Atlas Information Service, Nat. Res. Can., Ottawa, Ont. Canada, Plate 2.1.

Hwang, C. T. (1976), Predictions and observations on the behavior of a warm gas pipeline on permafrost, *Can. Geotech. J.*, *13*(4), 452–480.

Jorgenson, M. T., Y. L. Shur, and E. R. Pullman (2006), Abrupt increase in permafrost degradation in Arctic Alaska, *Geophys. Res. Lett.*, *33*, L02503, doi:10.1029/2005GL024960.

Kokelj, S. V., and C. R. Burn (2003), Ground ice and soluble cations in near-surface permafrost, Inuvik, Northwest Territories, Canada, *Permafrost Periglac.*, *14*, 275–289, doi:10.1002/ppp.458.

Kokelj, S. V., and C. R. Burn (2004), Tilt of spruce trees near ice wedges, Mackenzie Delta, Northwest Territories, *Arctic Alpine Res.*, *36*, 615–623.

Kokelj, S. V., and T. Jorgenson (2013), Recent advances in thermokarst research, *Permafrost Periglac.*, *24*, 108–119, doi:10.1002/ppp.1779.

Kokelj, S. V., M. J. F. Pisaric, and C. R. Burn (2007a), Cessation of ice-wedge development during the 20th century in spruce forests of the eastern Mackenzie Delta, Northwest Territories, Canada, *Can. J. Earth Sci.*, *44*, 1503–1515, doi:10.1139/e07-035.

Kokelj, S. V., C. R. Burn, and C. Tarnocai (2007b), The structure and dynamics of earth hummocks in the subarctic forest near Inuvik, Northwest Territories, Canada, *Arctic Alpine Res.*, *39*, 99–109.

Kokelj, S. V., D. Riseborough, R. Coutts, and J. Kanigan (2010), Permafrost and terrain conditions at northern drilling-mud sumps: Impacts of vegetation and climate change and the management implications, *Cold Regions Sci. Tech.*, *64*, 46–56.

Lachenbruch, A. H. (1962), Mechanics of thermal contraction cracks and ice-wedge polygons in permafrost, *Geol. Soc. Am. Spec. Pap.*, *70*, 1–66, doi:10.1130/SPE70-p1.

Lantz, T. C., and S. V. Kokelj (2008), Increasing rates of retrogressive thaw slump activity in the Mackenzie Delta region, N.W.T., *Geophys. Res. Lett.*, *35*, L06502, doi:10.1029/2007GL032433.

Lantz, T. C., S. E. Gergel, and S. V. Kokelj (2010), Spatial heterogeneity in the shrub tundra ecotone in the Mackenzie Delta region, Northwest Territories: Implications for Arctic Environmental Change, *Ecosystems*, *13*, 194–204, doi:10.1007/s10021-009-9310-0.

Mackay, J. R. (1963), *The Mackenzie Delta Area, N.W.T., Memoir 8*, 202 pp., Geograph. Branch, Dept. Mines Tech. Surv., Ottawa, Ont., Canada.

Mackay, J. R. (1970), Disturbances to the tundra and forest tundra of the western Arctic, *Can. Geotech. J.*, *7*, 420–432, doi:10.1139/t70-054.

Mackay, J. R. (1974), Ice-wedge cracks, Garry Island, Northwest Territories, *Can. J. Earth Sci.*, *11*, 1366–1383, doi:10.1139e/74-133.

Mackay, J. R. (1990), Some observations on the growth and deformation of epigenetic, syngenetic and anti-syngenetic ice wedges, *Permafrost Periglac.*, *1*, 15–29, doi:10.1002/ppp.3430010104.

Mackay, J. R. (1992a), Lake stability in an ice-rich permafrost environment: Examples from the western Arctic coast, in *Aquatic Ecosystems in Semi-Arid Regions: Implications for Resource Management*, National Hydrology Research Institute Symposium Series, vol. 7, edited by R. D. Robarts and M. L. Bothwell, pp. 1–6, Environment Can, Saskatoon, Sask., Canada.

Mackay, J. R. (1992b), The frequency of ice-wedge cracking (1967–1987) at Garry Island, western Arctic coast, Canada, *Can. J. Earth Sci.*, *29*, 236–248, doi:10.1139/e92-022.

Mackay, J. R. (1993), Air temperature, snow cover, creep of frozen ground, and the time of ice-wedge cracking, western Arctic coast, *Can. J. Earth Sci.*, *30*, 1720–1729, doi:10.1139/e93-151.

Mackay, J. R. (1995a), Ice wedges on hillslopes and landform evolution in the late Quaternary, western Arctic coast, Canada, *Can. J. Earth Sci.*, *32*, 1093–1105.

Mackay, J. R. (1995b), Active layer changes (1968 to 1993) following the forest-tundra fire near Inuvik, N.W.T., Canada, *Arctic Alpine Res.*, *27*, 323–336.

Mackay, J. R. (2000), Thermally induced movements in ice-wedge polygons, western Arctic coast: A long-term study, *Géogr. Phys. Quatern.*, *54*, 41–68.

Mackay, J. R., and S. R. Dallimore (1992), Massive ice of the Tuktoyaktuk area, western Arctic coast, Canada, *Can. J. Earth Sci.*, *29*, 1235–1249, doi:10.1139/e92-099.

Marsh, P., M. Russell, S. Pohl, H. Haywood, and C. Onclin (2009), Changes in thaw lake drainage in the Western Canadian Arctic from 1950 to 2000, *Hydrol. Process.*, *23*, 145–158, doi:10.1002/hyp.7179.

Molina-Giraldo, N., P. Bayer, P. Blum, and O. A. Cirpka (2011), Propogation of seasonal temperature signals into an aquifer upon bank infiltration, *Ground Water*, *49*(4), 491–502.

Morse, P. D., and C. R. Burn (2013), Field observations of syngenetic ice-wedge polygons, outer Mackenzie Delta, western Arctic Coast, Canada, *J. Geophys. Res. Earth Surf.*, *118*, 1320–1332, doi:10.1002/jgrf.20086.

Morse, P. D., C. R. Burn, and S. V. Kokelj (2009), Near-surface ground-ice distribution, Kendall Island Bird Sanctuary, western Arctic coast, Canada, *Permafrost Periglac.*, *20*, 155–171, doi:10.1002/ppp.650.

Murton, J. B. (1996), Thermokarst-lake basin sediments, Tuktoyaktuk Coastlands, western arctic Canada, *Sedimentology*, *43*, 737–760, doi:10.1111/j.1365-3091.1996.tb02023.x.

Murton, J. B., C. A. Whiteman, R. I. Waller, W. D. Pollard, I. D. Clark, and S. R. Dallimore (2005), Basal ice facies and supraglacial melt-out till of the Laurentide Ice Sheet, Tuktoyaktuk Coastlands, western Arctic Canada, *Quaternary Sci. Rev.*, *24*, 681–708, doi:10.1016/j/quascirev.2004.06.008.

Nixon, J. F. (1998), Recent applications of geothermal analysis in northern engineering, in *Proceedings of the 7th International Conference on Permafrost*, pp. 833–846, Centre. d'études nordiques, Univ. Laval, Ste.-Foy, Québec, Canada.

Nixon, J. F., and N. Holl (1998), Geothermal modeling of soil or mine tailings with concurrent freezing and deposition, *Can. Geotech. J.*, *34*, 234–250.

Oswell, J. M. (2011), Pipelines in permafrost: Geotechnical issues and lessons, *Can. Geotech. J.*, *48*, 1412–1431.

Palmer, M. J., C. R. Burn, and S. V. Kokelj (2012), Factors influencing permafrost temperatures across tree line in the uplands east of the Mackenzie Delta, 2004–2010, *Can. J. Earth Sci.*, *49*, 877–894, doi:10.1139/e2012-002.

Péwé, T. L. (1966), Ice-wedges in Alaaska—Classification, distribution, and climatic significance, in *Proceedings of the 1st International Conference on Permafrost, Lafayette, Indiana*, pp. 76–81, National Academy of Science Press, Washington, D. C.

Pollard, W. H., and H. M. French (1980), A first approximation of the volume of ground ice, Richards Island, Pleistocene Mackenzie Delta, Northwest Territories, Canada, *Can. Geotech. J.*, *17*, 509–516, doi:10.1139/t80-059.

Rampton, V. N. (1988), Quaternary geology of the Tuktoyaktuk Coastlands, Northwest Territories, GSC Memoir 423, 98 pp.

Romanovskii, N. N. (1985), Distribution of recently active ice and soil wedges in the USSR, in *Field and Theory; Lectures in Geocryology*, pp. 154–165, Univ. of British Columbia Press, Vancouver, BC.

Romanovsky, V. E., S. L. Smith, and H. H. Christiansen (2010), Permafrost thermal state in the polar Northern Hemisphere during the International Polar Year 2007–2009: A synthesis, *Permafrost Periglac.*, *21*, 106–116, doi:10.1002/ppp.689.

Smith, S. L., M. M. Burgess, D. Riseborough, and F. M. Nixon (2005), Recent trends from Canadian permafrost monitoring network sites, *Permafrost Periglac.*, *16*, 19–30, doi:10.1002/ppp.511.

Thornthwaite, C. W. (1948), An approach toward a rational classification of climate, *Geogr. Rev.*, *38*, 55–94.

Timoney, K. P., G. H. Laroi, S. C. Zoltai, and A. L. Robinson (1992), The high sub-Arctic forest-tundra of northwestern Canada: Position, width, and vegetation gradients in relation to climate, *Arctic*, *45*, 1–9.

Titus, R. L., and E. J. Truhlar (1969), A new estimate of average global solar radiation in Canada, Dept. of Transport, Meteorol. Branch, Climatol. Div. Climatic Data Sheet 7-69, Toronto.

Watanabe, T., N. Matsuoka, and H. H. Christiansen (2013), Ice- and soil-wedge dynamics in the Kapp Linné area, Svalbard, investigated by two- and three dimensional GPR and ground thermal and acceleration regimes, *Permafrost Periglac.*, *24*, 39–55, doi:10.1002/ppp.1767.

Williams, P. J., and M. W. Smith (1989), *The Frozen Earth: Fundamentals of Geocryology*, Cambridge Univ. Press, Cambridge, U. K.